Polyamide Nanocomposites with Improved Toughness

I. Kelnar, J. Kotek, L. Kaprálková, B. S. Munteanu

Institute of Macromolecular Chemistry, Academy of Sciences of the Czech Republic, Heyrovsky Sq. 2, 162 06 Prague 6, Czech Republic

Received 17 September 2004; accepted 19 August 2004
DOI 10.1002/app.21374
Published online in Wiley InterScience (www.interscience.wiley.com).

ABSTRACT: Polymer nanocomposites containing several percent of exfoliated layered silicates are materials with a unique weight/performance ratio. The only parameter that is not enhanced, but even decreased, is toughness. This work focused on the toughness enhancement of these advanced systems with polyamide matrix prepared via melt-mixing (i.e., by a conventional method of polymer processing having an advantage of easy simultaneous addition of other components). Analogously to ternary polyamide blends with improved mechanical behavior, containing finely and separately dispersed elastomer and rigid polymer, elastomer particles with an average size of 60 nm were incorporated in the nanocomposite. The very low particle size was achieved by *in situ* reactive compatibilization by using suitably functionalized elastomers. The simultaneously increasing viscosity of the system enhanced exfoliation of the silicate. Melt exfoliated nanocomposites containing 3 wt % of clay and 5 wt % of elastomer particles exhibit increased toughness without significant loss of other properties. Elastomer particles increase toughness by both acting as stress concentrators (by initiating energy absorbing microdeformations) and influencing the clay-induced matrix crystalline structure.
 J Appl Polym Sci 96: 288–293, 2005

Key words: polyamide 6; nanocomposite; toughness

INTRODUCTION

Polymer nanocomposites are engineering materials with a favorable weight–performance ratio, which often shows a far better combination of physical and mechanical properties than conventional microscale particulate composites.[1–3] The one property that mostly decreases (compared with the matrix value) is toughness.[3,4] Their unusual behavior is based on the influencing of physical and material parameters on a scale inaccessible by traditional filler materials. However, from length-scale arguments, it is known that toughening occurs in a specific size range,[5] and effective toughening may not be energetically favorable on nanolength scales. This process generally necessitates a filler size > 0.1 μm. Also enhancement of toughness found by the Argon group[6] due to the existence and overlapping of the crystalline layers with reduced resistance to shear flow around filler particles can be excluded in nanocomposites. In the case of polyamide 6 (PA6) nanocomposite, this layer is formed by the α crystals showing high anisotropy[7] in plastic deformation (parallel to filler surface), whereas, in the nanocomposite, instead of α form typical of neat polymer, the clay-induced less stable γ form also exists, with lamellae growing perpendicularly to the montmorillonite sheets,[8,9] which is apparently not favorable to toughening. The toughening mechanism mentioned above[6] also requires debonding at the interphase. Such a phase separation has not been observed in nanocomposites (e.g., a study dealing with AFM observation of fracture surfaces strongly confirms immobilized polymer chains on the clay surface).[10] Toughness enhancement was found only for nanocomposites with inherently brittle matrices such as epoxy resins or polyester resins,[10,11] especially in not fully exfoliated systems (i.e., those with larger intercalated domains).

In the case of nanocomposites with a ductile polymer matrix, mostly favorable properties of nanocomposites with fully exfoliated structure[4,11] are reported. On the other hand, when comparing exfoliated and intercalated systems with PA6 matrix, the exfoliated structure leads to the highest stress at break values, whereas intercalated structures exhibit the largest strain at break values.[8] Therefore, the intercalated structure, where polymer has entered into the galleries between silicates but has not fully delaminated them, offers some potential for toughening due to considerable interactions between silicate layers and a more favorable size-scale of intercalated domains. Liu et al.[12] have found an increase in toughness by the addition of 10% of maleated polypropylene (PP) to PA6 NC prepared via a polymerization technique.

Recently, we found a very good toughening effect[13,14] of a small amount ($\sim$ 5%) of very finely dis-

Correspondence to: I. Kelnar (kelnar@imc.cas.cz).
Contract grant sponsor: Grant Agency of the Czech Republic; contract grant number: 106/03/0679.

Part of this work was presented at the Second International Symposium on Polymer Nanocomposites Science and Technology, Boucherville, Canada.

persed rubber particles (average size, ~ 60 nm), when combined with similarly fine particles of a rigid (more so than the matrix) polymer in a pseudoductile semicrystalline matrix such as PA6 or poly(butylene terephthalate). Obtained results indicate different and more favorable behavior in comparison with both binary systems containing similarly fine particles[15] and ternary systems with larger, less bonded inclusions.[16] Of interest is the best efficiency at a relatively low total content of both components. Despite the fact that rigid particles can contribute to energy absorption by their plastic deformation,[17] due to relatively low gain[18] in toughness in system containing only these particles, more significant is the synergistic influence of stress fields induced by both rigid and elastomer inclusions. The goal of this work was to study the efficiency of fine well-dispersed elastomer particles on toughening of PA6 nanocomposites.

EXPERIMENTAL

Materials

The following materials were used: Cloisite 30B (Southern Clay Products, Inc., Gonzales, TX) montmorillonite modified with alkylbis (2-hydroxyethyl)methylammonium chloride alkyl derived from tallow (clay content 74 wt %); PA6 Ultramid B5 (BASF, Ludwigshafen, Germany), M_n = 42,000; poly(styrene-*co*-maleic anhydride) (SMA) Dylark 332, (Arco, Newton Square, PA), maleic anhydride content, 14%, M_n = 180,000; maleated (0.6%) ethylene-propylene elastomer (EPR-MA) Exxelor 1801, (Exxon Mobil, Köln, Germany); ethylene-propylene elastomer (EPR) Buna AP 331 (Degussa Hüls, Frankfurt, Germany); maleated (2%) styrene/ethene-butene/styrene copolymer (SEBS-MA) Kraton FX1901 (Ottignies-Louvain-La-Neuve, Belgium); ethylene-glycidyl methacrylate (6%) copolymer (PE-GMA), purchased from Aldrich; ethylene-methylacrylate-glycidyl methacrylate copolymer (E-MA-GMA) Lotader 8900 (Atofina, Carling, France); and ultrafine vulcanized butadiene-styrene rubber (Narpow VP 701), particle size 100–150 nm (Sinopec, Beijing, China).

Nanocomposite preparation

Prior to mixing, PA6 and clay were dried at 85 and 70°C, respectively, for 12 h in a vacuum oven. The blends were prepared by mixing the components in the W 50 EH chamber of a Brabender Plasti-Corder at 255°C and 45 rpm for 10 min. The material removed from the chamber was immediately compression-molded at 250°C to form 1-mm-thick plates. Strips cut from these plates were used for the preparation of dog-bone specimens (gauge length, 40 mm) in a laboratory microinjection molding machine (DSM). The barrel temperature was 265°C, and the mold temperature was 80°C. The reported values of clay content are wt % of Cloisite C30B and are not corrected for pure silicate content.

Testing

Tensile tests were carried out at 22°C by using an Instron 5800 apparatus at a crosshead speed of 20 mm/min. The stress-at-break, σ_b, elongation-at-break, ε_b, and Young's modulus, E, were evaluated. Experimental errors were 2, 15, and 5%, respectively.

Tensile impact strength, a_t, was measured with one-sided notched specimens, using a Zwick hammer with an energy of 4 J (experimental error 10–15%).

Dynamic mechanical analysis (DMA) was done in the single cantilever mode, using a DMA DX04T apparatus.

Morphological observations

Phase structure was observed by using a scanning electron microscopy (SEM) and cryofractured samples. The elastomer phases were etched with *n*-heptane for 1 h or with boiling xylene for 2 min. The size of dispersed particles was evaluated from their micrographs by using a MINI MOP image analyzer (Kontron Co., Germany). For transmission electron microscope (TEM) observations, ultrathin (60 nm) sections were cut under liquid N_2 from a stained (RuO_4 vapor for 90 min) samples by using a Leica Ultramicrotome UCT.

Wide-angle X-ray diffraction patterns (WAXS) were obtained by using a powder diffractometer HZG/4A (Freiberger Präzisionsmechanik GmbH, Germany) and monochromatic CuKα radiation.

RESULTS AND DISCUSSION

Mechanical properties

Figures 1 and 2 show the effect of increasing content of maleated EPR-MA on basic mechanical parameters of PA6 containing 5% of clay. The lowering of tensile strength and Young's modulus (E) is similar to a binary elastomer-containing blend.[19] Comparison of experimental E values with those calculated by using Kerner's model[20] (with modulus of single nanocomposite as matrix) shows a negative deviation for the real system with higher elastomer content. A possible negative effect of elastomer on exfoliation can be excluded (see below); the lower E is most probably a consequence of influencing crystallinity of PA6 by reactive elastomer.[18] On the other hand, the increase in elongation-at-break is relatively significant (in particular, the high value at 2% content), indicating a change in deformational behavior. Of importance is the similar enhancement of toughness. From these results, it is obvious that, in particular, the system

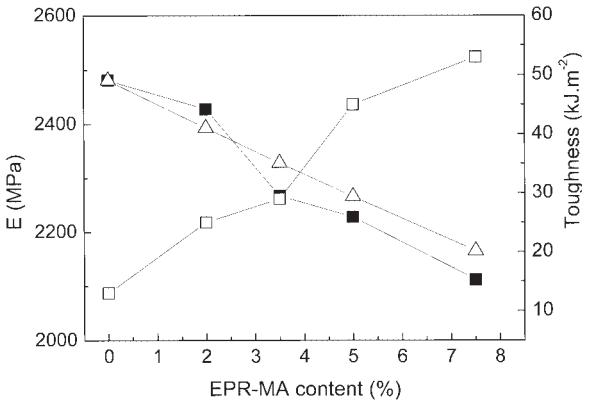

Figure 1 Dependence of modulus (■), E, Kerner model values (△), and tensile impact strength (□), a_t, on the EPR-MA content for PA6 with 5% of clay.

TABLE I
Dependence of Mechanical Properties on the Elastomer Type and Particle Size for System Containing 5% of Clay (C30B) and 5% Elastomer

Blend composition	σ_b (MPa)	E (MPa)	a_t (kJ m^{-2})	El. part. size (nm)
PA6	73.7	1620	16.5	—
PA6/C30B/EPR-MA	85	2228	45	60
PA6/C30B/SEBS-MA	81.5	2185	41	70
PA6/C30B/VP701	79.5	2281	31	120
PA6/C30B/EPR	83.2	2581	36	<1000
PA6/C30B/E-MA-GMA	75.6	2025	33	<200
PA6/C30B/PE-GMA	76	2080	25	<100
PA6/C30B/PP-MA[a]	82.9	2342	30	<500

[a] 10% of PP-MA.

containing 5% of clay and 5% of EPR-MA has an interesting balance of properties [i.e., stiffness and tensile strength are close to the unmodified nanocomposite (NC) values but toughness is significantly enhanced].

Effect of elastomer type

Table I shows the dependence of properties of the 90/5/5 PA6/clay/elastomer combination on the elastomer type. The best results were found for EPR-MA and SEBS-MA (i.e., a low modulus and well-dispersed rubber particles). The average particle size was lower than 100 nm (Table I, see also Fig. 8). The worsened properties of the system containing nonreactive EPR with larger particle size (<1 μm) confirm the importance of a very fine elastomer dispersion. The more rigid PE-GMA copolymer (shear modulus value, ~ 60 MPa in comparison with ~ 5 MPa for EPR-MA) is less effective for toughening despite having fine particles similar to EPR-MA. Low toughness was also found for ultrafine particles of vulcanized rubber, probably as a result of reduced deformability caused by crosslinking and also of lower adhesion to PA6 matrix due to the absence of compatibilization. We also prepared a system, similar to that published by Liu et al.,[13] where enhanced toughness was achieved by the addition of 10% PP-MA to a nanocomposite prepared via polymerization technique. The results in Table I show the toughness values lower than with 5% EPR-MA. Despite the addition of relatively rigid PP-MA, the stiffness was even more significantly reduced than for elastomer, probably due to a negative effect of reactive compatibilization on matrix crystallinity.[18]

The above results indicate the best effect is from ultrafine, well-bonded elastomer particles, similar to a PA6/rigid polymer/reactive elastomer combination.[14]

Effect of clay content

Properties of a neat PA6 matrix and of PA6 containing 5% EPR-MA were evaluated on their dependence on clay content. From Figure 3 is clear that the best tensile strength was found at the 5% clay content for both the nonmodified and the EPR-MA-containing nanocom-

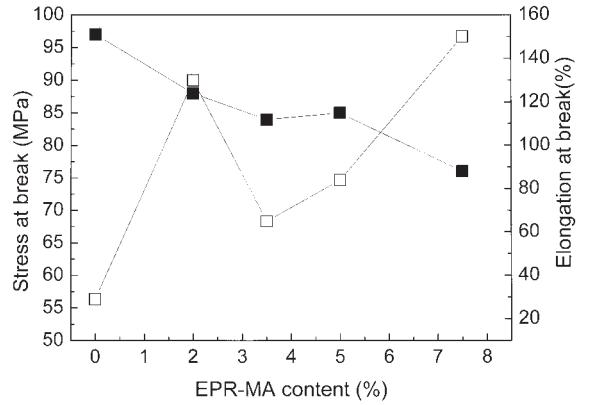

Figure 2 Dependence of stress at break (■), σ_b, and elongation (□), ε_b, on the EPR-MA content for PA6 with 5% of clay.

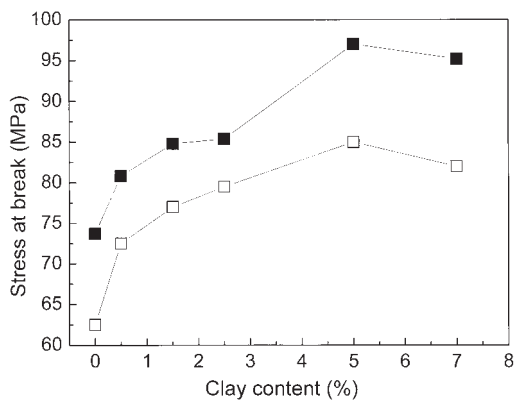

Figure 3 Stress at break of nanocomposites in dependence on the clay content (■) PA6 matrix, (□) PA6/EPR-MA 95/5 matrix.

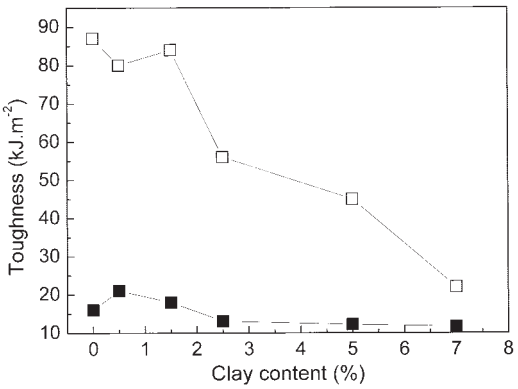

Figure 4 Tensile impact strength of nanocomposites in dependence on the clay content (■) PA6 matrix, (□) PA6/EPR-MA 95/5 matrix.

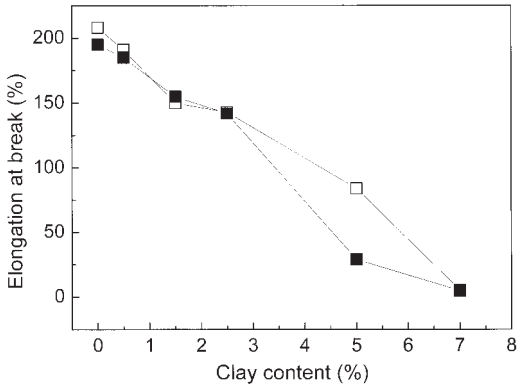

Figure 6 Elongation-at-break of nanocomposites in dependence on clay content (■) PA6 matrix, (□) PA6/EPR-MA 95/5 matrix.

posites. On the other hand, the toughness is markedly enhanced at lower clay contents (Fig. 4), but the material containing 5% of clay still exhibits significantly higher toughness than the matrix (and nonmodified NC). In the case of modulus (Fig. 5), the relatively more significant lowering by addition of elastomer (in comparison with Kerner's model values) also confirms the influence of matrix parameters by the added elastomer. This negative effect prevails especially at lower clay contents: with increasing clay content, the affecting of matrix properties by clay apparently dominates. This change in matrix morphology can also exclude a possible negative effect of EPR-MA on exfoliation, because this effect would more intensively deteriorate properties for higher clay contents. Rather unusual is a similar dependence of elongation at break (Fig. 6). Its values were very close, following the values of both matrices (PA6 and PA6/EPR-MA 95/5) without clay; a significant difference caused by elastomer was found for 5% clay content only. The above results indicate that for systems modified by EPR-MA, a very interesting balance of properties can be obtained, even at lower clay contents. For example, at 1.5% clay, the strength and modulus values are higher than those of neat PA6 and, at the same time, the toughness is significantly enhanced (7×).

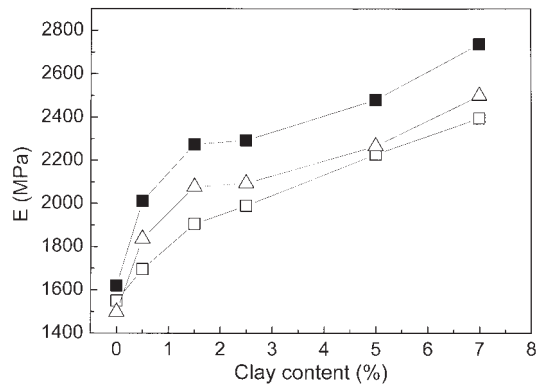

Figure 5 Young's modulus, *E*, of nanocomposites in dependence on clay content (■) PA6 matrix, (□) PA6/EPR-MA 95/5 matrix, (△) Kerner model values (experimental values of corresponding nanocomposite were used as matrix).

Morphology of deformed samples

The difference in micromechanical deformation behavior between nanocomposite and elastomer containing NC is obvious from SEM observations of fracture surfaces, where a higher extent of plastic deformation due to the presence of elastomer was found in comparison with analogous unmodified NC. This different behavior is even more visible from the structure of elongated neck, whereas in the NC [Fig. 7(a)], only the deformed structure exists without practically any voids. The presence of EPR-MA causes the formation of numerous voids [Fig. 7(b)], most probably due to cavitation of elastomer (or at least debonding, but this is less probable because of strong interfacial bonding of EPR-MA). On the other hand, practically no voids were found for the analogous system containing more rigid (see above) PE-GMA. These results indicate that low modulus elastomer is also able to initiate energy-absorbing processes in a system containing a well-exfoliated layered clay structure (see text below). At the same time, clay platelets probably provide stabilization of microdeformations caused by elastomer particles, similar to plastically deformed rigid polymer in the ternary blend.[21]

Effect of reactive elastomer on nanocomposite structure

TEM observations of EPR-MA containing NC (Fig. 8) show a high degree of clay exfoliation and also very fine elastomer particles. WAXS patterns (Fig. 9) indicate broader distribution of lamellar stacks in the presence of reactive components (EPR-MA or SMA) (i.e., a higher degree of exfoliation in comparison with single

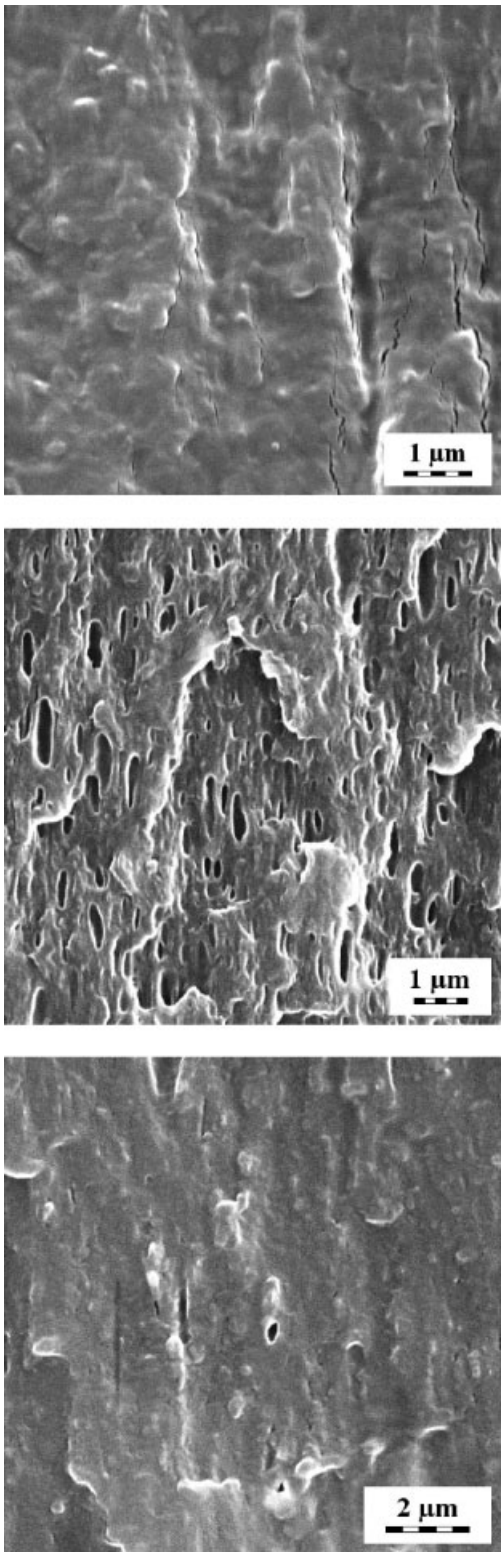

Figure 7 SEM observation of elongated neck (A) PA6 with 5% of clay, (B) 95/5 PA6/EPR-MA with 5% of clay, (C) 95/5 PA6/PEGMA with 5% of clay.

NC). This effect is a consequence of an increase in viscosity by the *in situ* compatibilizing reactions.

WAXS [Fig. 10(a)] results confirm the presence of a more stable γ-crystalline phase[22] (in comparison with

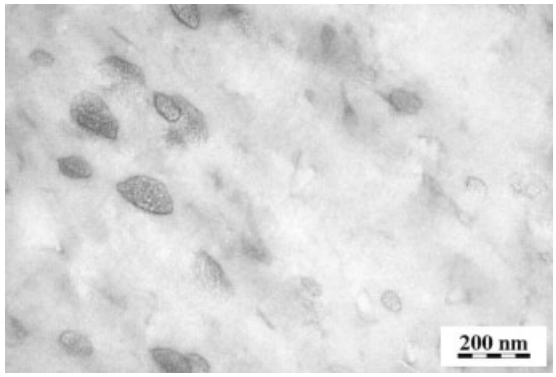

Figure 8 TEM picture of PA6 with 5% of clay and 5% of EPR-MA.

γ-phase in neat PA6) nucleated by the clay surface. Figure 10(b) shows the effect of a reactive elastomer on the stability of this phase. It is demonstrated that the γ-phase portion in the nanocomposite containing reactive elastomer was significantly reduced by thermal treatment at 130°C as compared with nonmodified NC. This means that the presence of reactive elastomer decreases the stability and character of the clay-induced γ-phase.

This fact is supported by DMA; the differences in the course of temperature dependencies of loss moduli (Fig. 11) for nonmodified and elastomer containing NC (higher E'' for elastomer containing NC below glass transition temperature, T_g) are a consequence of the expected disturbance of structures initiated by clay (e.g., possible influencing of γ-crystals).

Consequently, the more significant impact of the reactive component on stiffness in comparison with predicted values, mentioned above, originates predominantly from different PA6 matrix properties.

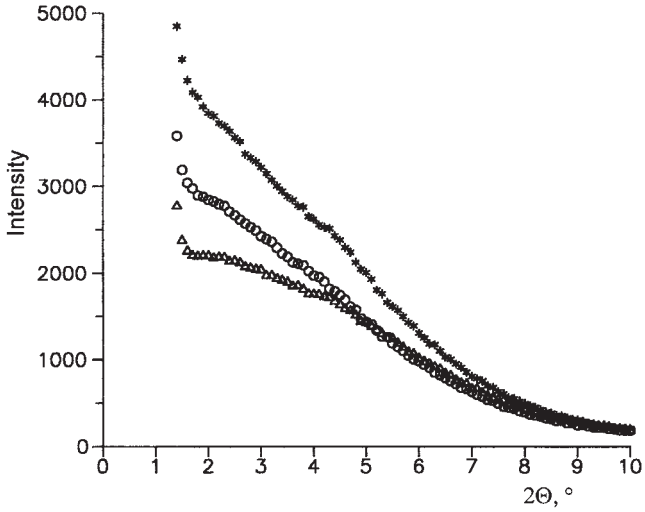

Figure 9 WAXS patterns of (△) PA/clay (bottom), (○) PA6/Clay/EPR-MA (middle), (*) PA6/clay/SMA (top).

CONCLUSIONS

The addition of a small amount of a finely dispersed elastomer can significantly enhance toughness of a nanocomposite without a remarkable loss in other properties. The presented results indicate that the elastomer is able to increase the energy-absorbing capacity of these systems by both acting as stress concentration sites and affecting properties (type and content of crystalline phase) of the matrix.

At the same time, variation of the elastomer and the clay content and/or ratio offers good potential to prepare a relatively wide range of systems with a very interesting balance of properties, which is not accessible with polymer blends and conventional microcomposites.

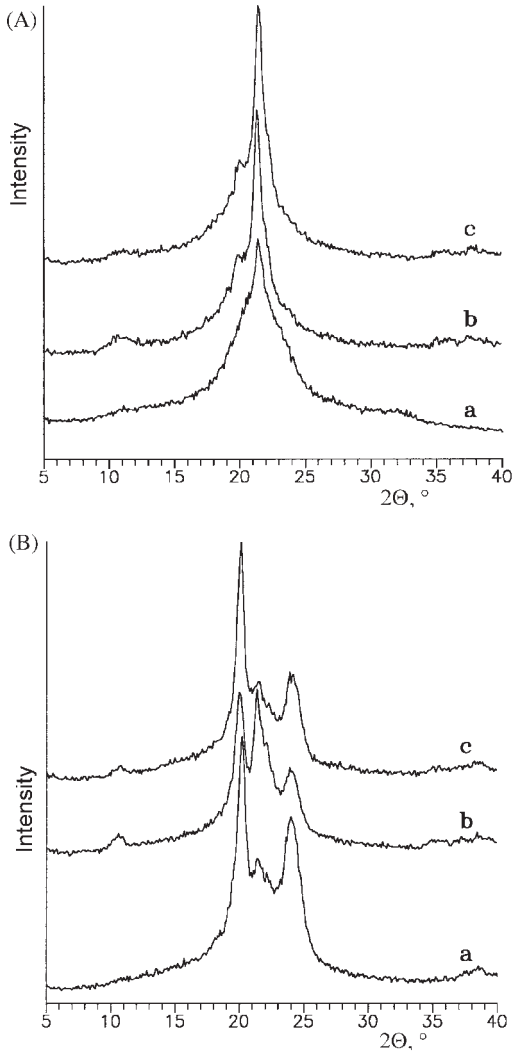

Figure 10 (A) WAXS patterns of curves: (a) PA6, (b) PA6/clay, (c) PA6/clay/EPR-MA; (B) the same samples after exposition 10 h at 130°C.

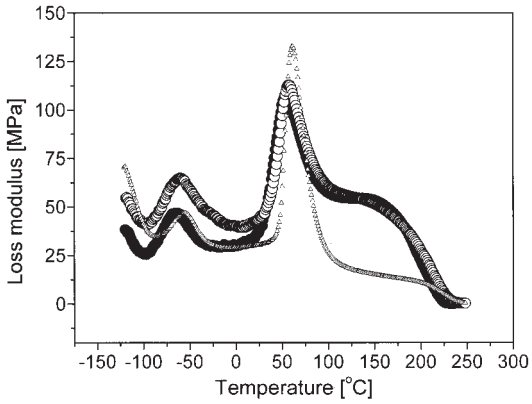

Figure 11 Temperature dependence of loss modulus of (●) PA6/clay, (○) PA6/clay/EPR-MA, (△) PA6.

References

1. Polymer-Clay Nanocomposites; Pinnavaia T. J.; Beall G. W., Eds.; Wiley: New York, 2001.
2. Liu, L.; Qi, Z.; Zhu, X. J Appl Polym Sci 1999, 71, 1133.
3. Jimenez, G.; Ogata, N.; Kavai, H.; Ogihara, T. J Appl Polym Sci 1997, 64, 2211.
4. Fornes, T. D.; Yoon, P. J.; Keskkula, H.; Paul, D. R. Polymer 2001, 42, 9929.
5. Bucknall, C. B. Toughened Plastics; Applied Science Publishers: London, 1977.
6. Bartczak, Z.; Argon, A. S.; Cohen, R. E.; Kowaleski, T. Polymer 1999, 40, 2367.
7. Masenelli-Varlot, K.; Reynaud, E.; Vigier, G.; Varlet, J. J Polym Sci, Part B: Polym Phys 2002, 40, 272.
8. Lincoln, D. M.; Vaia, R. A.; Wang, Z. G.; Hsiao, B. S; Krishnamoorti, R. Polymer 2001, 42, 9975.
9. Zerda, A. S.; Lesser, A. J. J Polym Sci, Part B: Polym Phys 2001, 39, 1137.
10. Kordmann, X.; Berglund, L. A.; Sterte, J; Giannelis, E. P. Polym Eng Sci 1998, 38, 1351.
11. Kojima, Y.; Usuki, A.; Kawasumi, M.; Okada, A.; Fukushima, Y.; Kurauchi, T., Kamigaito, O. J Mater Res 1993, 8, 1185.
12. Liu, X.; Wu, Q.; Berglund, L. A.; Fan, J.; Qi, Z. Polymer 2001, 42, 8235.
13. Kelnar, I.; Stephan, M.; Jakisch, L.; Fortelný, I. Polym Mater Sci Eng 1988, 79, 206.
14. Kelnar, I.; Stephan, M.; Jakisch, L.; Fortelný, I. J Appl Polym Sci 2000, 78, 1597.
15. Borggreve, R. J. M.; Gaymans, R. J.; Schuijer, R. J.; Ingen Housz, J. F. Polymer 1987, 28, 1489.
16. Kelnar, I.; Fortelný, I. J Polym Eng 1995, 14, 269.
17. Kurauchi, T.; Ohta, T. J Mater Sci 1984, 19, 1699.
18. Kelnar, I.; Stephan, M.; Jakisch, L.; Fortelný, I. J Appl Polym Sci 1997, 66, 555.
19. Gaymans, R. J. In Polymer Blends; Paul D. R.; Bucknall, C. B., Eds.; Wiley: New York, 2000; Vol. 2, Chapter 25.
20. Kerner, E. H. Proc Phys Soc 1956, 69, 808.
21. Kelnar, I.; Kotek, J.; Munteanu, B. S.; Fortelný, I. J Appl Polym Sci 2003, 89, 3647.
22. Maiti, P.; Okamoto, M. Macromol Mater Eng 2003, 288, 440.